Pasquale Cavaliere *Editor*

Laser Cladding of Metals

Springer

Laser Cladding of Metals

Pasquale Cavaliere
Editor

Laser Cladding of Metals

Springer

Editor
Pasquale Cavaliere
Department of Innovation Engineering
University of Salento
Lecce, Italy

ISBN 978-3-030-53194-2 ISBN 978-3-030-53195-9 (eBook)
https://doi.org/10.1007/978-3-030-53195-9

This Springer imprint is published by the registered company Springer Nature Switzerland AG
The registered company address is: Gewerbestrasse 11, 6330 Cham, Switzerland

Preface

Laser cladding (LC) for additive manufacturing is a very interesting process for both the production industry and research. Today, LC challenges process engineers and material scientists with many adjustable processes and material parameters, metallurgy, and defects. The development of laser cladding with its unique advantages will continue to advance with additive manufacturing of complex functional and volumetric parts. Additive manufacturing through laser cladding is a nonlinear process depending on many variables. Many models have been developed in order to predict the optimal cladding properties as a function of the fundamental processing parameters governing the deposition. The online continuous process monitoring is fundamental for the final quality of the laser cladded structures. Although laser cladding process is currently well controlled from a manufacturing strategy point of view and allows producing healthy components with a low or nonexistent porosity level, the microstructure of the parts obtained by these techniques is far from being understood and controlled. In metals, the grain size and orientation are essential factors for the control of the properties, especially the mechanical properties. The type of solidification (columnar or equiaxed) and grain size depend on the local solidification conditions, while the grain orientation is strongly conditioned by epitaxy phenomena based on the current orientation of the substrate microstructure. It is therefore very important to be able to model the behavior of the metal during its solidification and to be able to predict what type of solidification will occur. The goal is to correlate the main parameters of this additive manufacturing process with the microstructure generated by them and relate them to the mechanical properties obtained from samples.

The introductory chapters of the book illustrate the potential of Laser Cladding Technology as an optimal additive manufacturing tool. Laser cladding has evolved into a potent three-dimensional additive manufacturing technology by stacking the deposited material layers. Currently, a wide variety of materials can be processed. The ability to functionalize surfaces as well as 3D-printed objects leads to further integration of structural, optomechanical, and thermal properties into these parts. One approach is the combination and encapsulation of optical elements like quartz lenses or laser crystals with custom alloys, thus creating multi-material components.

Additive manufacturing with laser cladding also offers the opportunity to integrate cooling solutions, which reduce mechanical stresses and improve optical properties of the assemblies. These complex structures lead to increasingly complex processes with narrow process and parameter windows within which defects can occur. Several materials can be employed for the production of laser cladding coatings in order to achieve high hardness for wear resistance, thermal and corrosion barriers, and fatigue life improvement.

The book's chapters are devoted to illustrate the model employed for production of the optimal microstructure of laser cladded components. The main aim is to correlate the main parameters of this additive manufacturing process with the microstructure generated by them and relate them to the mechanical properties obtained from samples.

Many examples on laser-cladded superalloys, titanium alloys, and steel are provided. The specific relationship among composition, processing parameters, corrosion, and mechanical properties in laser cladding technology are described.

My special acknowledgments to the passion and cooperation of all the authors and reviewers who made possible the realization of this book and the reduction of the publication time with their hard work and prompt responses. My special thanks to the professionalism of the editorial office manager and assistants.

Lecce, Italy Pasquale Cavaliere

Contents

Nomenclature

3D	Three-Dimensional
AM	Additive Manufacturing
BCC	Body-Centered Cubic
BF	Bright Field
BM	Base Metal
BS	Building Strategy
CAD	Computer Aided Design
CAFE	Computer-Aided Fabrication Environment
CET	Columnar to Equiaxed Transition
CGLs	Continuous Galvanizing Lines
CNC	Computer Numerical Controlled
CS	Cold Spray
CT	Computed Tomography
CTL	Constant Track Length
DEM	Discrete Element Modeling
DF	Dark Field
DMD	Direct Metal Deposition
DMLD	Direct Metal Laser Deposition
DSR	Deep Surface Rolling
DTL	Decreasing Track Length
EDS	Energy Dispersive Spectroscopy
EHLA	Extreme High-Speed Laser Material Deposition
EIS	Electrochemical Impedance Spectra
EMS	Electromagnetic Stirring
ERDF	European Regional Development Fund
FCC	Face-Centered Cubic
FEA	Finite Element Analysis
FEM	Finite Element Modelling
FESEM	Field Emission Scanning Electron Microscopy
fHAp	Fluorapatite
FWR	Fatigue Wear Resistance

GFA	Glass Forming Alloys
GTAC	Gas Tungsten Arc Cladding
HA	Hydroxyapatite
HAZ	Heat Affected Zone
HCP	Hexagonal Close Packed
HEA	High Entropy Alloy
HPDL	High-Power Diode Lasers
IBJs	Insulated Block Joints
IE	Incident Energy
LACS	Laser-Assisted Cold Spray
LAM	Laser Additive Manufacturing
LAMPR	Laser Additive Manufacturing Process Replicator
LC	Laser Cladding
LCD	Laser Cladding
LDMD	Laser Direct Metal Deposition
LENS	Laser Engineered Near Net Shaping
LOF	Lack of Fusion
LPBF	Laser Powder Bed Fusion
LR	Laser Remelting
LSFed	Laser Solid Formed
LSFF	Laser Solid Freeform Fabrication
LST	Laser Surface Treatment
MERC	Materials and Energy Research Center
MMCs	Metal Matrix Composites
MP	Melting Pool
MRI	Magnetic Resonance Imaging
PBF	Powder Bed Fusion
PHT	Post-Heat Treated
PID	Proportional-Integral-Derivative
PLD	Pulsed Laser Deposition
PVA	Polyvinyl Alcohol
RA	Regression Method
RCF	Rolling Contact Fatigue
SBF	Simulated Body Fluids
SCE	Saturated Calomel Electrode
SEBM	Selective Electron-Beam Melting
SFE	Stacking Fault Energy
SGs	Stray Grains
SLD	Supersonic Laser Deposition
SLM	Selective Laser Melting
SMAW	Shielded Metal Arc Welding
SLS	Selective Laser Sintering
SX	Single-Crystal
TBC	Thermal Barrier Coating
TEM	Transmission Electron Microscopy

TGO	Thermally Grown Oxide
TZ	Treated Zone
WG	Water Glass
XRD	X-Ray Diffraction

Chapter 1
Laser Cladding – Additive Manufacturing

Robert Bernhard, Philipp Neef, Henning Wiche, Volker Wesling, Christian Hoff, Jörg Hermsdorf, and Stefan Kaierle

1.1 Introduction to Additive Manufacturing with Laser Cladding

After the discovery of laser technology in 1960, the precision and flexibility of lasers showed great potential for material and surface processing. Due to the high initial costs and the low efficiency of laser beam sources, it took laser cladding until the 1980s to become adopted industry-wide (Corbin et al. 2004). It proved to be a promising alternative to conventional electric arc welding and cladding methods, since the confined heat input results in low dilution and an overall reduction of defects (Morgado and Valente 2018).

At its core, laser cladding is a laser welding process where individual weld beads are aligned and stacked onto a substrate material. In its simplest form, it is used to clad metal surfaces with metals or carbides. Typical applications are the reinforcement of mechanical parts that are used in abrasive or corrosive environments (Lachmayer et al. 2018). The cladding of ductile round stock with a hard and wear-resistant metal improves tribological properties of gears and bearings. Compared to other cladding processes, the laser-based process is very flexible and therefore the higher investment for the laser source is often worthwhile. Additive manufacturing with laser cladding evolved with the need for the repair of worn drawing dies for metal stamping (Levy et al. 2003). In addition, reinforcement of structures with increased complexity used in the automobile industry is possible.

Generally, laser cladding process heads exist in two different configurations, which themselves are distinctive in wire and powder-based filler material. At the

R. Bernhard (✉) · P. Neef · H. Wiche · V. Wesling
Clausthaler Zentrum für Materialtechnik, Clausthal-Zellerfeld, Germany
e-mail: r.bernhard@lzh.de

C. Hoff · J. Hermsdorf · S. Kaierle
Laser Zentrum Hannover e.V., Hannover, Germany

P. Cavaliere (ed.), *Laser Cladding of Metals*,
https://doi.org/10.1007/978-3-030-53195-9_1

same time, both systems can be designed with an off-axis or a coaxial material supply (Lammers et al. 2018).

Laser metal deposition in pure cladding applications is typically set up for maximum deposition rates. Therefore, large amounts of wire or powder filler material are added to the laser processing zone off-axially. For sophisticated additive tasks with higher resolution, a coaxial powder or wire nozzle setup is required.

One of the main advantages of laser cladding for additive manufacturing is the large build volume, where some build-chambers can have the size of multiple cubic meters. The possibility to add onto existing freeform surfaces allows the combination of high-speed conventional machining and specialized additive manufacturing.

Advances in process development enable not only changing complexity, but also the use of special and even hard to weld materials. Laser cladding is not only limited to metals, even ceramics or carbides can be used to disperse into metal surfaces to functionalize 3D-printed parts.

Leveraged through advanced process monitoring and feedback control loops, even larger objects with longer print durations and ultimately safety-relevant aviation parts can be manufactured and repaired.

1.2 Laser Cladding Setup for Additive Manufacturing

A typical laser cladding machine for additive manufacturing consists of a laser source, a processing head, a numeric control, and an enclosure. Material can be added in the form of a wire or a powder feed. The necessary laser power depends on the material and the targeted deposition rate. Typically, 0.5–3 kW near-infrared diode, fiber, or disk lasers are used. The machine presented here has a 680 W diode laser, six independent axes of movement and a build volume of 1000 × 1500 × 1000 mm (W×H×D). It is equipped with a coaxial powder-based processing head. For process control, a pyrometer and a computer-vision system is in place (see Fig. 1.1).

Starting from the laser beam source, the laser light is guided to the process head via an optical fiber. There, the beam propagates through a converging lens that collimates the beam. The beam is reflected at a dichroitic mirror at a 45° angle. The mirror is transmissive for the pyrometer and the camera wavelength. The combined process and sensor beams are focused on a substrate. The work piece is melted locally and through an annular nozzle. Shield gas and metal powder are added coaxially. Moving the process head results in weld beads, which can be oriented in x and y direction. Volumetric buildup is created by stacking layers and remelting previously printed material.

Materials that can be processed by laser cladding are manifold. The main requirement is availability as powder or wire, depending on the used technique. One of the advantages of powder-based materials is that the material composition can easily be modified (see Fig. 1.2) (Neef et al. 2019). Even in situ alloys of incompatible materials like metals and ceramics can be achieved. Printable, atomized metal powder

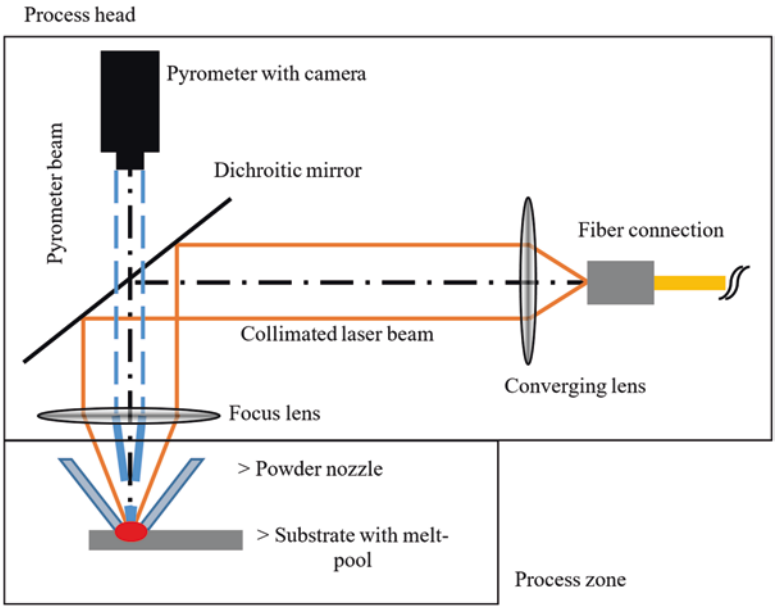

Fig. 1.1 Schematic drawing of a laser cladding process head (Bernhard et al. 2019b)

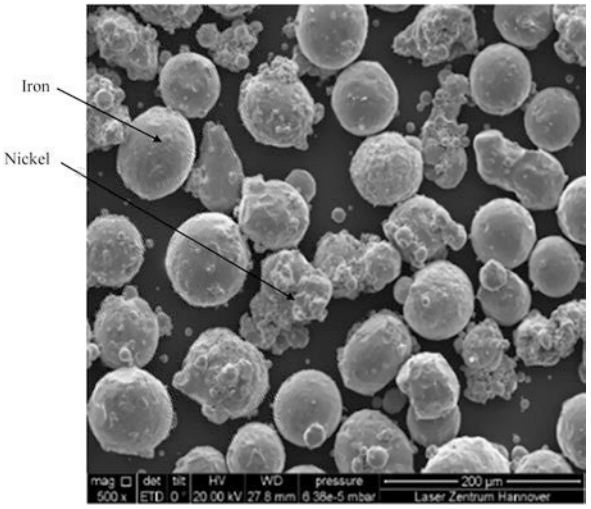

Fig. 1.2 Iron–nickel powder (Bernhard et al. 2019a)

can range from structural steel to special nickel superalloys like CMSX-4 and PWA 1426 (Alfred et al. 2018). Furthermore, due to the fine control of the powder mass-flow, high-resolution parts can be manufactured. In contrast, wire-based laser cladding processes are used for coarser structures. It is a cleaner process since less material is lost by powder overspray. Generally, metal wires are available at lower

Table 1.1 Overview of common materials for laser cladding

Material	Remarks
Structural steel	Mahamood (2018)
Composites	
Nickel-based superalloys	Alfred et al. (2018) and Kaierle et al. (2017)
Cobalt	Brueckner et al. (2017) and Mueller (2019)
Titanium	
Copper	
Molybdenum	Bernhard et al. 2019a, b
Iron–nickel	
316 L steel	Trumpf (2019)
Aluminum	
Bronze	

costs, but with its fixed metallurgic composition, variations of additives can only be done by coating the surface of the wires (Gehling et al. 2019). Powder properties like particle size and distribution in conjunction with their morphology dictate the flowability of the powder due to possible interlocking of individual grains. Compared to powder bed processes, laser cladding is less sensitive to variations of these properties and allows for heterogeneous powder compositions.

An overview of common additive manufacture materials can be seen in Table 1.1.

1.3 Process Parameters of Laser Cladding

Process parameters of laser cladding continue to be the subject of research. Parameter windows are strongly influenced by the material, the substrate, and the geometry of the printed objects. The results of laser cladding are very dependent on the process parameters. One of the most significant parameter sets is the laser power P (W) and the feed rate f (m/s). Their relation is described as linear energy E = P/f (J/m) and it dictates the energy input and therefore the size of the melt pool. Additionally, the amount of powder added to the process zone mainly impacts the resulting deposition rate and temperature of the melt-pool. The feed rate of the processing head has an influence on the process time and the overall volumetric heat input regarding the size of the heat-affected zone and the dilution of the metals. Another main factor is the material used and its inherent properties. These include the melting point, weldability, surface tension of the liquid phase, thermal conductivity, and reflectivity/absorption of laser light.

Furthermore, different parameters can become significant in specific circumstances. In situations where heat dissipation is restricted at, for example, quick geometric changes, the type and flow rate of the shielding gas can become critical. The large number of parameters is a challenge for the process development.

Table 1.2 Iron–nickel parameters for additive manufacturing

Laser power	Laser spot diameter	Laser M^2	Feed rate	Hatch distance
272 W	0.84 mm	115	180 mm/min	0.6 mm
	Top hat			
Layer height	**Standoff distance**	**Powder mass-flow**	**Carrier gas-flow**	**Mean grain size**
0.1 mm	9 mm	2.2 g/min	5000 cm^3/min	60 µm

For a deeper insight into the process and in search of best parameters, the application of design of experiments is indispensable. As an example, the process parameters for additive manufacturing of iron–nickel powder are shown in Table 1.2. These parameters were found by the use of a statistical screening design and a subsequent full factorial design of experiments.

1.4 Power-Based Laser Cladding with its Limitations and Possibilities

Laser cladding has many advantages, including the generation of parts that are not manufacturable by conventional processes, due to their complex shapes, gradual material composition, or undercuts. The powder nature of the filler material and steep thermal gradients can lead to unwanted changes in microscopic and macroscopic appearances. Especially powder processes like laser cladding for additive manufacturing and laser powder bed fusion (LPBF) are prone to defects inside the 3D printed metal (Zhang et al. 2017). The application of novel but hard to weld materials results in increasingly complex processes with narrow process and parameter windows. Inevitably, defects can occur during the print process. Irregularities of a laser cladding process can range from small pores to larger heat-induced cracks as well as bonding defects and cavities, as shown in Fig. 1.3. Bonding defects are typically a result of insufficient energy input that results in elongated pores. Pores are gas-filled, whereas cavities and cracks are a result of shrinkage.

Inclusions inside the printed part can range from segregation to impurities and oxidation. Oxidation is a challenge due to the large build volume that only allows for local inert atmospheres. During the process, oxygen can react with the heated material and form unwanted oxides. This can lead to microscopic defects and irregularities. Another common macroscopic error is a lack of dimensional accuracy. The thermal capacity changes with every layer; especially at corners, the heat is concentrated. An additional limitation for 3D printing is the compromise between complexity and deposition rate. Fine structures with a resolution of 100 µm are possible with powder-based laser cladding. At this resolution, the deposition rate decreases to 0.5–1 g per minute (Kaierle et al. 2012). Larger focus diameters reduce the fidelity significantly but allow deposition rates up to 10 kg/h.

To counteract these defects, efforts are being made to mitigate these effects and make the process more robust. Controlled process environments monitored with

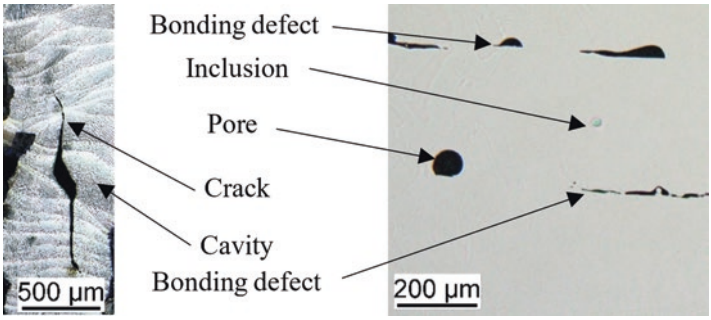

Fig. 1.3 Laser cladding defects visible in a microsection (Bernhard et al. 2019b)

Fig. 1.4 Computer-vision melt-pool identification (a, b), FFT of acoustic emissions (c)

different sensors are key to a reliable and repeatable process. Developments in computing power allow fast image processing of the melt pool. From the captured melt-pool image, the contour is extracted and a convex hull is superimposed (see Fig. 1.4a, b). In-process evaluation of temperature, shape, area, stability, and uniformity with feedback control to the powder mass-flow, feed rate, and laser power greatly improve the printed results. These data in conjunction with acoustic and deposition measurements allow the creation of a visual representation of the data (see Fig. 1.4c).

1.5 Creation of Multi-Material Components

Development is not only limited to the process itself. Newly developed material combinations and even gradient compositions allow the manufacturing of functional parts never seen before. Furthermore, new possibilities include the combination of optical thermal and structural components, where material groups with opposing properties can be combined by specific material adaptation (Neef et al. 2019). Using the additive design freedom, especially multi-material components with laser active materials could benefit from this. In Fig. 1.5, a 3D-printed multi-

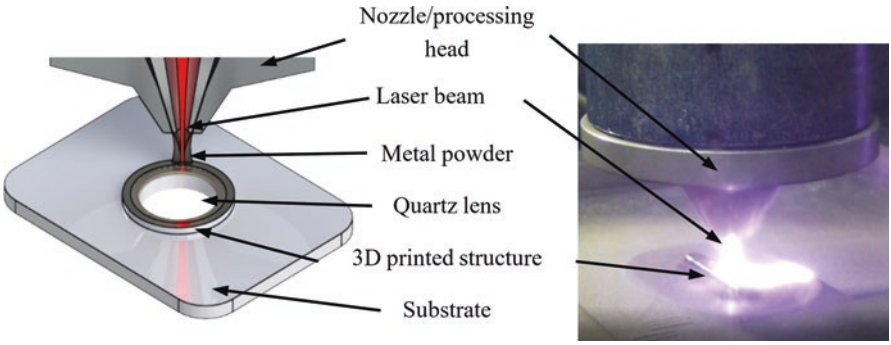

Fig. 1.5 Multi-material processing with additive laser cladding (Bernhard et al. 2019a)

material lens mount is shown. An integration of cooling channels, reducing the part count, bionic, lightweight construction for space applications, and full automation are just some of the future project goals that can be achieved by laser cladding.

1.6 Conclusion and Outlook

Laser cladding for additive manufacturing is a very interesting process for both the production industry and research. In the past 30 years, it has evolved to a robust and very flexible additive process at reasonable costs. Today it challenges process engineers and material scientists with many adjustable process and material parameters, metallurgy, and defects. At the same time, demands for complex, function-integrated, and individualized parts are increasing. Multifunctional and multi-material parts open up the opportunity to cover that demand and are subject to research. Eventually, by sampling process emissions, it will be possible to visualize and qualify the process for safety-related applications. Therefore, the development of laser cladding with its unique advantages will continue to advance with additive manufacturing of complex functional and volumetric parts.

Acknowledgments We thank the Ministry for Science and Culture of Lower Saxony and the European Regional Development Fund (ERDF) for the funding and support.

Duration of implementation: 01.07.2018 – 30.06.2021.

Project number: ZW6-8501 8048 (wGROTESK).

References

Alfred, I., Nicolaus, M., Hermsdorf J., Kaierle, S., Möhwald, K., Maier, H.-J., & Wesling, V. (2018). *Advanced high pressure turbine blade repair technologies*. CIRP conference on photonic technologies (LANE 2018).

Bernhard, R., Neef P., Wiche, H., Wesling, V., Hoff, C., Hermsdorf, J., & Kaierle, S. (2019a). *Process development for additive multi-material components*. 2019 Lasers in manufacturing conference Munich.

Bernhard, R., Neef P., Wiche, H., Wesling, V., Hoff, C., Hermsdorf, J., & Kaierle, S.. (2019b). *Defect detection in additive manufacturing via a toolpath overlayed meltpool-temperature tomography*. 2019 ICALEO conference, Orlando.

Brueckner, F., Riede, M., Mueller, M, Marquardt, F., Knoll, M., Willner, R., Seidel A., Lopéz E., Leyens C., & Beyer E. (2017). *Fabrication of metallic multi-material components using laser metal deposition*. Solid Freeform Fabrication Symposium.

Corbin, S., Khajepour, A., & Toyserkani, E. (2004). *Laser cladding*. Boca Raton: CRC. ISBN 978-1-4200-3917-7.

Gebhardt, A. (2013). *Generative Fertigungsverfahren: Additive Manufacturing und 3D Drucken für Prototyping – Tooling – Produktion*. Munich: Carl Hanser Verlag.

Gehling, T., Treutler, K., & Wesling, V. (2019). Targeted influence on the weld strength of high-strength fine-grain structural steels in the GMA welding process through functionalized weld material surfaces. *Welding in the World, 63*, 783–792. https://doi.org/10.1007/s40194-019-00707-2.

Kaierle, S., Barroi, A., Noelke, C., Hermsdorf, J., Overmeyer, L., & Haferkamp, H. (2012). Review on laser deposition welding: From micro to macro. *Physics-Procedia, 39*.

Kaierle, S., Overmeyer, L., Alfred, I., Rottwinkel, B., Hermsdorf, J., Wesling, V., & Weidlich, N. (2017). Single-crystal turbine blade tip repair by laser cladding and remelting. *CIRP Journal of Manufacturing Science and Technology, 19*, 196–199.

Lachmayer, R., Lippert, R. B., & Kaierle, S. (2018). *Additive Serienfertigung – Erfolgsfaktoren und Handlungsfelder für die Anwendung*. Berlin/Heidelberg: Springer.

Lammers, M., Budde, L., Barroi, A., Hermsdorf, J., & Kaierle, S. (2018). Entwicklung von Laser-Systemkomponenten optimiert für die additive Fertigung mittels SLM. In *Konstruktion für die additive Fertigung*. Berlin/Heidelberg: Springer.

Levy, G. N., Schindel, R., & Kruth, J. (2003). Rapid manufacturing and rapid tooling with layer manufacturing (LM) technologies. *CIRP Annals, 52*.

Mahamood, R. M. (2018). *Laser metal deposition process of metals, alloys, and composite materials*. Cham: Springer. ISBN: 978-3-319-64984-9.

Morgado, T., & Valente, C. (2018). *Development status of LASER Cladding and the new metallic alloys.* https://doi.org/10.20944/preprints201805.0417.v1

Mueller, M. (2019). Metallische Werkstoffe – Pulvertechnologie. *Fraunhofer-Allianz Generative Fertigung*. https://www.generativ.fraunhofer.de/en/research/materials.html. Retrieved 15 October 2019.

Neef, P., Bernhard, R., Wiche, H., Wesling, V., Kranert, F., Budde, J., Wienke, A., Neumann, J., Kracht, D., Lammers, M., Ahlers, H., Grabe, T., Rettschlag, K., & Lachmayer, R. (2019). *Generatives Fertigen optischer, thermaler und struktureller Komponenten für Lasersysteme, NSM 2019/Clausthal-Zellerfeld/Shaker Verlag*. ISBN: 978-3-8440-6471-1.

TRUMPF. (2019). Maschinen AG, Marco Ritz. https://www.technische-rundschau.ch/site/assets/files/44977/09_ritz_kopie.pdf. Retrieved 15 October 2019.

Zhang, B., Li, Y., & Bai, Q. (2017). *Defect formation mechanisms in selective laser melting: A review*. Berlin/Heidelberg: Springe.

Chapter 2
Additive Manufacturing by Laser Cladding: State of the Art

P. Cavaliere, A. Silvello, and A. Perrone

2.1 Introduction

Recently, large research and industrial attention has been devoted to additive manufacturing technologies based on direct energy deposition. High-quality materials coatings with good metallurgical bonds and minimal heat input into the work piece can be achieved by laser cladding through powder or wire feeding.

Many materials can be employed for laser cladding coatings production in order to achieve high hardness for wear resistance, thermal and corrosion barriers, fatigue life improvement. The quality of laser cladded structures is largely influenced by processing parameters (Shim et al. 2016). The authors addresses methods for selecting an appropriate layer thickness setting, which is an important parameter in layer-by-layer deposition manufacturing. A new procedure is proposed for determining the layer thickness setting for use in slicing of a part based on the single-layer height for a given depositing condition. The power, the scanning speed, and the material feeding are the fundamental parameters that can be tuned during processing and they have the largest impact on the final quality of the deposited structure. They all influence the single-layer height while the layer width is mainly governed by the scanning speed, power, and spot size. The laser cladding operational window can be defined in terms of laser power P [W], laser beam scanning speed S [mm/s], and powder feeding rate F [mg/s]. These are the three key parameters as they can be easily controlled and have a strong effect on the final outcome of the clad layer. A complete description of the cladding process is complex as it also depends on additional parameters such as laser beam spot size, laser beam energy distribution,

P. Cavaliere (✉) · A. Perrone
Department of Innovation Engineering, University of Salento, Lecce, Italy
e-mail: pasquale.cavaliere@unisalento.it; angelo.perrone@unisalento.it

A. Silvello
Thermal Spray Centre (CPT), Dto. CMiQF, Universitat de Barcelona, Barcelona, Spain
e-mail: asilvello@cptub.eu

P. Cavaliere (ed.), *Laser Cladding of Metals*,
https://doi.org/10.1007/978-3-030-53195-9_2

carrier and shielding gas used, how exactly the powder is fed, etc. Difficulty with the description of the process is due to many different interactions and various physical phenomena (Nenadl et al. 2014). The key quantities are: the amount of powder provided per unit length of the laser track F/S and the total heat input per unit length of the laser track P/S. It has been shown experimentally that over a wide range of processing parameters, the clad height, H, depends linearly on the F/S parameter with the laser power having a minimal effect. Similarly, the width, w, of the laser track linearly depends on $P/S^{1/2}$ and the clad area, Ac, is controlled by the $P^{1/2}*F/S$ parameter. These empirical dependencies were observed for both, side and coaxial cladding setups with high values of the correlation coefficient ($R > 0.9$) for cladding of Ni- and Co-based coatings on iron-base substrates.

2.2 Materials for Laser Cladding

Different materials behave differently, because of their melting temperatures, surface tension, and specific heat capacities differences. In addition to these inherent physical properties, different materials require different thermal management strategies in order to control, for example, hardening and crack formation. These effects require tailoring of process parameters to each new material processed. Also, since the geometry of the deposit and the fixture used will affect the thermal dissipation and buildup of temperature, process parameters might have to be adjusted during deposition depending on the specific deposit and fixture. High temperature resistant materials are normally selected for laser cladding coatings. For this reason, the whole microstructural and mechanical behavior at high temperature is fundamental for their potential application. Focusing on Co-based alloys, Eutroloy 16,006 was deposited showing clads without pores or cracking retaining high hardness up to 525 °C (de Oliveira et al. 2006). Stellite SF6 was deposited with preheating the substrate at 650 °C in order to avoid cracking and optimize residual stresses. The coating showed hardness up to 880 HV with diffusion of Fe from the substrate leading to improvement in wear and corrosion properties (Jendrzejewski et al. 2008). If thermally cycled at 1050 °C, a strong modification of carbides morphology and precipitation is revealed (d'Oliveira et al. 2002). Tribaloy® T-800 shows similar hardness levels, though its high-temperature corrosion susceptibility limits the application ranges (Navas et al. 2006). Diaz et al. (2012) have proved not only the possibility of performing coatings to repair or improve the properties of the Cr-Mo ASTM A182 F11 steel, but also the fact that these layers can be obtained by means of the laser cladding process. Dendritic microstructures and free crack and porosity coatings were achieved in the case of Stellites® and Tribaloy® T-900, keeping original properties of coating and substrate. Only Tribaloy® T-800 presents crack formation. Preheating of substrate can reduce this tendency of cracking but not completely remove its formation.

The damage of die surface due to cyclic thermo-mechanical loading is detrimental to the service life. In order to enhance the die life, it has been observed that

cladding-based repair is superior to welding or thermal spraying repair techniques. In this study, experimental study of laser cladding of H13 has been carried out. CPM 9 V steel powder has been deposited on H13 tool steel plate for repairing the die surface damage using a CW CO2 laser in conjunction with powder injection system. The effect of laser parameters on clad geometry and clad quality has been investigated (Kattire et al. 2015). The hard vanadium carbide particles increase the clad hardness to an average of four times greater than the substrate hardness. It has been observed that compressive residual stresses are generated in clad, which is desirable for repair applications as it will impede the crack propagation resulting in enhanced die life.

To strengthen Invar alloy, nanostructured carbide-strengthened cobalt-based cladding layers were fabricated on an Invar alloy by laser cladding. The cladding layers contained cubic γ-(Fe, Ni) or Co-based solid solution and hard carbides such as W_2C, Cr_3C_2/V_8C_7, CoCx, and niobium carbide at the grain boundaries. The cladding layers improved the wear and oxidation resistance of the Invar alloy without changing its coefficient of thermal expansion. The results indicated that the friction coefficient of composite coatings decreased by 28.6% compared with that of Invar substrate (Zou et al. 2020). An in situ synthesized high-volume fraction WC-reinforced Ni-based composite coating was fabricated on a mild steel substrate by using a high-power diode laser. Three kinds of single-layer coatings of different amounts of W + C powder and Ni60 powder and a five-layer coating with different amounts of W + C and Ni60 powders in each layer were prepared. This work showed that the multilayer coating possesses the highest hardness among all coatings, and the maximum hardness of the coatings was about 3.7 times more than that of the substrate. The gradient coating technology combined with the feature that WC particles were liable to sink in the bottom of coating were employed as a new idea for preparing the composite coating free of pores and cracks (Shu et al. 2017).

Stellite 6 was deposited by laser cladding of two different chromium-bearing steel substrates (P91 and P22). The results showed less cracking and pore development for Stellite 6 coatings applied to the P22 steel substrate. Further, the Stellite coating on P22 steel was significantly harder than that deposited on the P91 steel. The wear test results showed that the weight loss for the coating on P22 steel was significantly lower than for the P91 steel substrate. The surface topography data showed that the surface roughness for the coating on P22 steel was much lower than for the P91 steel substrate. It is concluded that the residual C content for the deposit on P22 was higher, mainly because the lower concentration of strong carbide formers, compared to P91, reduced the extent of carbon loss in the deposit (Kusmoko et al. 2014).

NiCrAl-based coatings are optimal for high-temperature protection (De Damborenea et al. 1994). Thanks to the formation of ceramic and metallic oxides on the surface of the specimen, which prevent the spread of alloy elements toward the exterior, and the entry of oxygen into the material, the coating exhibits superior high-temperature corrosion resistance. NiCrBSi coatings show very high wear resistance at high temperatures (Guo et al. 2011). Hardness increases with higher concentrations of B, C, Cr, and Si (Conde et al. 2002). Laser cladding NiCrBSi/

WC-Ni composite coating shows better high-temperature wear resistance than NiCrBSi coating, which is due to the formation of hard WC phase in the composite coating. NiCr coatings show a degradation of properties around 600 °C (Yang et al. 2012). Results indicated that the laser clad NiCr/Cr_3C_2 coating consisted of Cr7C3 primary phase and γ-(Fe,Ni)/Cr_7C_3 eutectic colony, while the coating added with WS_2 was mainly composed of Cr_7C_3 and (Cr,W)C carbides, with the lubricating WS_2 and CrS sulfides as the minor phases. The wear tests showed that the friction coefficients of two coatings both decrease with the increasing temperature, while both the wear rates increase. The same behavior is described for NiMoSi coatings (Lu and Wang 2004). Aging of the coating at 800 °C leads to gradual dissolution of the interdendritic eutectic Mo_2Ni_3Si and subsequent formation of a dual-phase structure with equiaxed Mo_2Ni_3Si primary grains distributed in the NiSi single-phase matrix. Because of the strong covalent-dominated atomic bonds and high volume fraction of the ternary metal silicide Mo2Ni3Si, both the original and the aged Mo_2Ni_3Si/NiSi coating has excellent wear resistance under pin-on-disc, high-temperature sliding wear test conditions; although hardness of the aged coating is slightly lower than that of the As-clad coating. NiCrAlY-based coatings show stability up to 1100 °C (Partes et al. 2008). The obtained results suggested that up to 450 h the system was able to form a continuous alumina layer that could protect the substrate from oxygen diffusion. The Fe addition can easily be accomplished in laser cladding process by dilution of the Tribaloy® T-800 coating with the steel substrate. In this work, a comparative study of microstructure, hardness and cracking susceptibility of low and high diluted T-800 and T900 coatings deposited by laser cladding is presented. A lower cracking ratio is obtained for the T-900 coatings at the cost of a lower hardness and wear resistance. No noticeable effect on the cracking susceptibility of the T-800 is found due to dilution with the substrate. However, a change in its microstructure is observed giving superior hardness and wear resistance (Tobar et al. 2008). Intermetallic coatings have good high-temperature wear resistance under sliding wear test conditions (Chen and Wang 2004). The laser clad chromium-alloyed nickel silicide coating has a rapidly solidified microstructure consisting of the Ni2Si primary cellular-dendrites and minor amount of interdendritic Ni2Si/NiSi eutectics. The intermetallic coating has good wear resistance under dry sliding wear test conditions due to the high hardness, refined microstructure, and strong intermetallic atomic bonds (Cai et al. 2003). The LC of single-tracks and 3D (three-dimensional) objects of the Ni3Al intermetallic was successfully prepared. Good metallographic characteristics and interface bonding were obtained. The coating microstructure consisted of γ-Ni3Al. The cladding of the Ni3A1 coating with small dilution into substrate can be obtained only at the appropriate power density of about 2–8 J/mm2 under the laser scan velocity of 100–200 mm/min and the powder feed rate ~ 3.8 g/min. The average micro-hardness of the laser cladded coatings was HV0,1380–1400. The ability of the multilayer LC process to build the Ni3Al intermetallic coatings was successfully shown (Kotoban et al. 2014).

Under high-temperature oxidation tests performed in air furnace at 1100 °C up to 200 h, weight gain of NiCoCrAlY was significantly larger than those of Ni and

CoNi alloy counterparts, and 50 times less than the weight gain of the substrate. This can be understood as a consequence of its larger Al content. Surface morphology was inspected by SEM-EDS, revealing a dense, stable, and continuous Al_2O_3 oxide layer with Ni, Co, Cr, and Y oxide inclusions. The percentage of these oxides is as low as 5% in the NiCoCrAlY coating, reaching about a 50% in the CoNiCrAlY one (Tobar et al. 2014).

By analyzing the deposition of Inconel718 powders, increasing the laser power and decreasing the scanning speed has shown to significantly increase the width of the deposit bead, whilst increasing the powder feeding rate and decreasing the scanning speed has shown to significantly increase the height of the deposit bead. Additionally, a decreased laser standoff distance and increased laser power significantly increased the penetration depth. The top surface straightness was significantly affected by the powder standoff distance where an increased positive distance increased the deviation in the top surface. The microstructure was mainly columnar with long dendrites growing epitaxially in the height direction. However, in the top surface there was a thin section with a dendritically equiaxed structure. This structure was most probably formed due to a lower thermal gradient and the increase of solidification velocity caused by the convection with the shielding gas (Segerstark 2015).

Results indicate the use of laser cladding technique as an alternative to plasma spray or HVOF methods, yielding fully dense coatings with metallurgical bonds to substrate. According to the effect of the three factors on bonding strength, the powder type has the largest dependency, followed by scanning speed. The laser output power has minimal impact. The bonding strength with iron-based powder is much higher than that with the nickel-based powder. The bond strength increases as the laser power increases. No obvious dependence of bonding strength on scanning speed has been found (Xu et al. 2015). Based on the background of the engineering application of automobile mold repair and surface strengthening, the effects of process parameters on the formation and microstructure of laser cladding nickel(Ni)-based alloy coating were studied (Yufan et al. 2020). The optimal parameters were: laser power 2000 W, powder feeding rate 15 g/min, scanning speed 4 mm/s. Under this process, the cladding layer and the substrate can exhibit good metallurgical bonding, and the cladding layer has fine crystal grains and a low dilution ratio. On this basis, different mass fractions of niobium carbide (NbC) powder were added to the nickel-based powder and laser cladding was carried out on the surface of die steel. The results show that with the increasing of niobium carbide addition, the hardness of the cladding layer decreases, and the wear loss of the cladding layer decreases first and then increases. When the niobium carbide addition reaches 6 wt.%, the wear loss of the cladding layer is the least, and the wear resistance is the best.

Surface modification of Ti-6Al-4 V is necessary surface to enhance its tribological properties. Multi-phase and multi component coating development is one of the present research trends in surface engineering arena. In Dhanda et al. (2014) it was attempted to develop a multi-component coating by laser cladding process using a pre-placed powder mixture containing Ni5Al (50 vol%) + hBN (10 vol%) + B4C

(20 vol%) + SiC (20 vol%) on substrate of Ti-6Al-4 V to improve its tribological performance. A nanostructured coating was formed with micro-hardness (780 HV0.05). X-ray diffraction (XRD) identified the presence of compounds like TiC, BN, TiB2, SiC, and intermetallics of Ni-Ti in the coating. The wear behavior of the composite coating was assessed by ball-on-disc type wear and friction monitor at 10 N load at 300 RPM taking a track diameter of 5 mm. Specific wear rate and coefficient of friction (μ) were found to vary from 0.6E-12 to 2.2E-12 m3/N-m and from 0.15 to 0.45, respectively, due to rubbing of coated surface against tungsten carbide ball.

Metal matrix composite (MMC) coatings were fabricated on Ti–6Al–4 V titanium alloy by laser cladding. Co42 self-fluxing powder, B4C, SiC, and Y2O3 were employed as the cladding materials. Results showed that the laser cladding coatings were mainly reinforced by CoTi, CoTi2, NiTi, TiC, TiB2, TiB, Cr7C3, and Ti5Si3. The micro-hardness of the cladding coatings was equivalent to three to four times the Ti–6Al–4 V substrate. Laser cladding coating exhibiting outstanding wear resistance was fabricated with the addition of 20 wt.% B4C, 7 wt.% SiC, and 1 wt.% Y2O3. The wear resistance was enhanced by over ten times compared with the substrate (Weng et al. 2020).

2.3 Clad Geometry

The precise prediction of the clad geometry as a function of the employed processing parameter per each used material is fundamental for additive manufacturing applications such as 3D printing. Many studies report the correlation between the cladding and the processing parameters (Chan et al. 1999). In Narang et al. (2012), the outputs from the welding, such as the weld macrostructure characteristics, were mathematically modeled with respect to the input process variables. Based on the weldment characteristics, including that of the bead contact angle, a mapping technique was developed for the graphical representation of the macrostructure zones' shape profiles. Taking into account the complexity of the laser cladding process governed by the heat transfer among the laser beam, the substrate and powder, and mass transfer between the powder flow and the molten surface, many authors suggest that the best approach should be based on "combined parameters" (Felde et al. 2002). This phenomenological approach uses simple mathematical formulae, derived from a statistical analysis of measured data, to relate the laser cladding parameters with the geometric features of the clad track. Given the required clad height and available laser beam power, the proposed method allows one to calculate values of the scanning speed and powder feed rate, which are used to obtain low dilution, pore-free coatings, fusion bonded to the substrate. Different sets of combined parameters are proposed to predict the track width and height for coaxial and lateral geometry of the powder feeder (De Hosson et al. 2009). In Toyserkani et al. (2003), the proposed model can predict clad geometry as a function of time and process parameters including beam velocity, laser power, powder jet geometry, laser

pulse shaping, and material properties. Suryakumar et al. (2011) modeled the formations of single beads and overlapping multiple beads. While the individual bead's geometry is influenced by the size of the filler wire and the speeds of the wire and torch, the step over increment between the consecutive beads additionally comes into the picture for the multiple bead deposition. So, the geometry prediction is possible over many process windows for both powders and wire-based laser cladding techniques. In Hoadley and Rappaz (1992), a two-dimensional (2D) finite element model is presented for laser cladding by powder injection. The model simulates the quasi-steady temperature field for the longitudinal section of a clad track. It takes into account the melting of the powder in the liquid pool and the liquid/gas free surface shape and position, which must conform to the thermal field in order to obtain a self-consistent solution. The model shows the linear relationship between the laser power, the processing velocity, and the thickness of the deposited layer. Another simplified model was proposed by Picasso et al. (1994). For a given laser power, beam radius, powder jet geometry, and clad height, this model evaluates two other processing parameters, namely, the laser-beam velocity and the powder feed rate. It considers the interactions between the powder particles, the laser beam, and the molten pool. In Naveed Ahsan and Pinkerton (2011) a coupled analytical–numerical solution is presented. Submodels of the powder stream, quasi-stationary conduction in the substrate and powder assimilation into the area of the substrate above the liquidus temperature are combined. An iterative feedback loop is used to ensure mass and energy balances are maintained at the melt pool. The knowledge of temperature, velocity, and composition distribution history is essential for a better understanding of the process and subsequent microstructure evolution and properties. Numerical simulation not only helps to understand the complex physical phenomena and underlying principles involved in this process, but it can also be used in the process prediction and system control. The double-track coaxial laser cladding with H13 tool steel powder injection is simulated using a comprehensive three-dimensional model, based on the mass, momentum, energy conservation, and solute transport equation. Some important physical phenomena, such as heat transfer, phase changes, mass addition and fluid flow, are taken into account in the calculation. The physical properties for a mixture of solid and liquid phase are defined by treating it as a continuum media. The velocity of the laser beam during the transition between two tracks is considered. The evolution of temperature and composition of different monitoring locations is simulated (He et al. 2009). Bax et al. (2018) offers guidelines to evaluate process parameter maps for single tracks, which are a requirement for high-quality claddings and 3D structures. The procedure is executed creating a process map for the parameters laser power, powder feed rate, and scanning speed. The relationship between process parameters and output responses and the interaction among the process parameter are analyzed and discussed in detail for Ti6Al4V. The analysis results indicate that powder feed rate is the dominant factor on the width and height of cladding coating while laser scanning speed has the strongest effect on molten depth of substrate (Sun and Hao 2012). The correlations that exist between key parameters of the process (i.e., laser power, scanning speed, powder feeding rate) and geometrical characteristics for single clads (i.e., height,

width, dilution, and wetting angle) were predicted and analyzed by regression method (RA). The preliminary geometrical considerations allowed to choose the processing parameters that led to high-quality clads with minimum porosity. All considerations finally resulted in the development of a processing map that shows the optimum parameters for laser cladding process (Erfanmanesh et al. 2017). The influence of the laser power, scan speed, and laser beam focal position (focus, positive and negative defocus) on the shape factor, cladding-bead geometry, cladding-bead microstructure (including the presence of pores and cracks), and hardness has been evaluated. The correlation of these process parameters and their influence on the properties and, ultimately, on the feasibility of the cladding process, is demonstrated. The importance of focal position is demonstrated. The different energy distribution of the laser beam cross section in focus plane or in positive and negative defocus plane affects the cladding-bead properties (Riquelme et al. 2016). Ti–6Al–4 V deposits with variable thickness are made to assess the use of laser cladding as a repair technology. Both the effect of the building strategy (BS) and the incident energy (IE) on the metallurgical characteristics of the deposits in relation to their complex thermal history have been studied. It is shown that for the configuration consisting in a decreasing track length (DTL) under high IE, a gradient of cooling rate exists that leads to the presence of different phases within the microstructure. Conversely, homogeneous microstructures are present either for the configuration with a constant track length (CTL) under high IE, and for the strategy obtained from a DTL under low IE (Paydas et al. 2015). Francis (2017) analyzed three different process parameters, power, velocity, and spot size, on melt pool geometry for the electron beam wire feed and laser powder feed processes of Ti6Al4V. Beam spot size has been identified as having a major influence on melt pool geometry. It was also shown that experimental melt pool dimensions can be used to estimate how spot size changes with a focusing parameter in additive manufacturing processes. Increases in spot size have been shown to eliminate the presence of keyholing, and a normalized spot size threshold is proposed to prevent keyholing in five alloys.

Many experimental evidences demonstrate how the cladding properties depend on the substrate material. In Kumar and Roy (2009), a three-dimensional conduction heat transfer model is developed to predict the clad geometry (e.g., height, width, and dilution) and microstructure (scale and morphology) of the solidified layer for a laser cladding process. The effect of controllable input process parameters like absorbed laser power, powder deposition rate, and processing speed on the clad characteristics is critically assessed with the help of dimensionless parameters. A process map is developed that enables operators to pick up the proper process parameters for a feasible laser cladding process with desirable characteristics. Li and Ma (1997) found that the surface roughness (turbulence) of an overlapped cladding layer decreased with the increase of the overlapping ratio in an oscillating manner. At some overlapping ratios the turbulence was at minimum and at some other ratios it was at maximum. Among various single-track sections, overlapping with symmetrical parabolic section single-clad tracks produced the smoothest cladding layer, in which the surface turbulence decreased in an oscillating manner. Lalas

et al. (2007) have taken into account the process speed and feed rate of the powder being supplied for the estimation of clad geometry. The surface tension between the added material and the substrate is used primarily for the calculation of the clad characteristics.

To obtain the powder packing information in the powder bed, dynamic discrete element modeling (DEM) was used (Lee 2015). The results show that negatively skewed particle size distribution, faster scanning speed, low power and low packing density worsen the surface finish quality and promote the formation of balling defects.

In El Cheikh et al. (2012), a mathematical model implemented in the software Mathematica 8© is used to predict the clad cross-section dimensions and obtain an analytical description of the clad geometry. It was experimentally noticed that the cross-section shape is a disk due to the surface tension forces. Analytical relationships are established between the radius and the center of the disk on the one hand and the process parameters on the other hand.

During the layer additive manufacturing, the cross-sectional profile of a single weld bead as well as overlapping parameters is critical for improving the surface quality, dimensional accuracy, and mechanical performance. Xiong et al. (2013) highlights an experimental study carried out to determine the optimal model of the bead cross-section profile fitted with circular arc, parabola, and cosine function, by comparing the actual area of the bead section with the predicted areas of the three models. A necessary condition for the overlapping of adjacent beads is proposed. The results show that different models for the single bead section profile result in different center distances and surface qualities of adjacent beads. The optimal model for the bead section profile has an important bearing on the ratio of wire feed rate to welding speed.

Laser cladding using scanning optics is a relatively little studied matter. Scanning optics makes the adjustment of laser beam interaction zone numerically possible and it is, therefore, a more flexible optical tool than the conventional static optics. A series of cladding tests were conducted using a 5 kW fiber laser and an oscillating linear scanner with dynamic powder feeding to determine the process characteristics and their possibilities and limitations (Pekkarinen et al. 2012). It was noticed that by using scanning optics, it is possible to vary the width and thickness of clad beads on a large scale. With scanning optics, it is possible to affect clad bead geometry so that only a 20% overlapping ratio is used. However, certain cladding parameter combinations expose the clad bead to cladding defects. Also, a fast moving scanned laser beam causes a wave formation to the melt pool that further causes stirring in the melt pool. The dilution was increased with increase in the cladding speed. However, the increase of the dilution was dependent on the scanning amplitude.

Modification of the cladding angle during overlap has been observed experimentally and linked with the formation of an inter-run porosity. There is another group of models of laser cladding process that try to model all physically involved processes, involving some approximation in equations and solve these numerically. Physical phenomena including heat transfer, melting, and solidification phase

changes, mass addition, and fluid flow in the melt pool, were modeled in a self-consistent manner. Interactions between the laser beam and the coaxial powder flow, including the attenuation of beam intensity and temperature rise of powder particles before reaching the melt pool were modeled with a simple heat balance equation. The level-set method was implemented to track the free surface movement of the melt pool, in a continuous laser cladding process. The governing equations were discretized using the finite volume approach. Temperature and fluid velocity were solved for in a coupled manner (Qi et al. 2006). Laser beam cladding of metals by single-step powder delivery is analyzed with a process model that is based on balance equations of energy and mass. Effects like powder heating, clad layer formation, substrate dilution and overlapping of tracks are discussed in dependence of the process parameters. In particular, the powder catchment efficiency and the beam energy redistribution in the material can be optimized by the powder mass flow rate and by the geometrical properties of the beam and of the powder jet (Kaplan and Groboth 2001). A three-dimensional finite element model is presented for precisely simulating laser cladding process with a focus on dilution control (Zhao et al. 2003). Dilution is referred to as an important quality index in the laser cladding process, indicating the contamination level of the properties of clad layer by substrate metals. As regards a good quality of laser clad layer, low dilution as well as metallurgical bond of interface are prerequisite, so the dilution control is essential in the process.

2.4 Textures and Microstructure Evolution

The rapid solidification (in the order of 10^3 K/s) produces many different microstructures in the laser cladded materials. So, the relationships between processing parameters and the final microstructure as well as properties of laser clad coatings are very complex. Conventional chill casting as well as laser surface cladding were used to produce a wide range of solidification Stellite 6 microstructures (Frenk and Kurz 1994). A detailed microstructural study of Stellite 6 coating deposited on a low carbon ferritic steel substrate using preplaced powder method and low-power Nd:YAG pulse laser was performed by Farnia et al. (2013). The shape of solidification front during pulsed laser cladding is similar to the shape of solidification front during continuous cladding with a doubled laser beam scanning speed. Further, OIM reveals the Greninger–Troiano OR between the face centered cubic coating and bcc substrate grains. It is concluded that at the moment of solidification, epitaxial growth of the grains in the coating occurs on the austenitic grains of the substrate and that an austenite–ferrite transformation occurs in the heat-affected zone upon subsequent cooling. High cooling rates during laser cladding of stainless steels may alter the microstructure and phase constitution of the claddings and consequently change their functional properties. Hemmati et al. (2011) showed that an extreme refinement of the solidification structure will influence the phase constitution of the coatings by lowering the Ms (Martensite start) temperature and hence stabi-

lizing the austenite, which results in lower hardness values and increased wear rates in AISI 431 steel. These results confirm that the structural refinement obtained by higher cladding speeds is not helpful for improving the hardness and wear properties of laser-deposited martensitic stainless steel coatings. The single-track formation and the deposition of block sample from 316 L stainless steel powders have been carried out by both SLM and LCD techniques. A comparison on pool shape, cooling rate, columnar grain size and mechanical properties under different processing conditions by LCD and SLM respectively has been studied. It is found that, due to the increase of energy input and the decrease of depth-to-width ratio of melting pool (MP) from SLM to LCD, the primary cellular arm spacing (PCAS) of the sample increases from less than 1.0 μm to more than 15.0 μm, and thus the cooling rate of MP decreases from about 10 K/s in SLM to about 10 K/s in LCD. Furthermore, due to the decrease of cooling rate from SLM to LCD, the columnar grains of the as forming alloy are getting coarser (Ma et al. 2017). The samples of 316 L stainless steel by SLM have much stronger tensile strength but lower elongation than those by LCD, and the main reason is due to the fact that the solidification behavior of the MPs by SLM can form much finer columnar grains than those by LCD.

Alvarez et al. (2018) summarize the influence of the most relevant process parameters in the laser cladding processing of single and compound volumes (solid forms) made from AISI 316 L stainless steel powders and using a coaxial nozzle for their deposition. Process speed, applied laser power, and powder flow are considered to be the main variables affecting the laser cladding in single clads, whereas overlap percentage and overlapping strategy also become relevant when dealing with multiple clads. By setting appropriate values for each process parameter, the main goal of this study is to develop a processing window in which a good metallurgical bond between the delivered powder and the substrate is obtained, trying simultaneously to maintain processing times at their lowest value possible.

The experimental work carried out has consisted in the verification of the viability of three iron-based materials AISI 4340, AISI 430 L, and DIN 16MnCr5 for repair processes using EHLA. For this, an experimental process consisting of four work packages was carried out: (1) analysis of the deposition of a layer of material to select the laser power and feedforward that give low porosity and no bonding defects; (2) selection of the nozzle displacement according to the thickness obtained in the analysis of a layer by the deposition of blocks of five layers; (3) preliminary study of 3 mm to see the behavior of the material in greater thicknesses and choose the best manufacturing strategy; and lastly, (4) buildup of 10 mm samples (Edurne 2018).

The evolution of macro- and microstructures of laser-deposited Al–Si samples was investigated by Dinda et al. (2012). Microstructural observation revealed that the morphology and the length scale of the microstructures are different at different locations of the sample. A periodic transition of microstructural morphology from columnar dendrite to microcellular structure was observed in each layer. Cloots et al. (2016) investigated selective laser melting (SLM) of the nickel-based superalloy IN738LC and the cobalt-based alloy Mar-M509, and identify the influence of process and material parameters on the resulting microstructure. Significant differ-